On the Equivalence of Multi-Agent 2D Coverage Control and Leader-Follower Consensus Network

Xiaotian Xu[1], Alexander Davydov[2], and Yancy Diaz-Mercado[1]

***Abstract*— Coverage control algorithms seek to spatially distribute agents in a domain of coverage, e.g., to minimize proximity to all points. Leader-follower consensus network algorithms use local coordination rules to influence the behavior of a multi-agent system (MAS) as a whole through explicit control of a subset of agents (called leaders) and neighbor interactions. In this paper, the equivalence of these two classes of distributed algorithms for swarm robotics, that were once considered inherently different, is established. We present a swarm robotics application, where the real agents (i.e., the robots) in the domain of coverage are followers; and virtual agents (i.e., the leaders) are introduced based on the domain of coverage. The dynamics of followers are shown to be in the form of a weighted, state-dependent consensus protocol and the dynamics of the leaders (dependent on the evolution of the domain) are provided. Formulating a standard coverage algorithm (i.e., Lloyd's algorithm) over 2D polygonal domains as a leader-follower consensus protocol makes the structure of the ensemble-level dynamics for the MAS explicit with respect to neighbor interaction. The resultant weighted graph Laplacian may contribute to the future investigation on the performance guarantees of a MAS tracking a time-varying domain. The equivalence of the two classes of algorithms is validated in simulation.**

I. Introduction

Coverage control of multi-agent systems (MASs) [1] deploys a group of agents in the space to collaboratively complete tasks such as surveillance or exploration of a region of interest. Among all the coverage control strategies, the standard decentralized coverage control law is the continuous-time version of Lloyd's algorithm [2]. Coverage algorithms are considered as a mechanism of coordinating many agents which has been leveraged in many applications including human-swarm interaction [3], [4], translation and shaping control of MASs [5], [6], persistent environment monitoring [7], [8], and pursuit-evasion games [9], [10]. However, in most of these cases the domain of interest is static. For time-varying domains, a family of decentralized control laws is derived in [5], but convergence guarantees are only obtained in the fully centralized case. Tracking error bounds for Lloyd's algorithm over time-varying 1D manifolds has been investigated in [11] by representing Lloyd's algorithm as a leader-follower network [12] with time-invariant graph Laplacian matrix. However, the guarantees for a MAS to track a reference input (e.g., time-varying domains), i.e., the bound of the tracking error dynamics, for coverage control algorithms in $\mathbb{R}^d, d \geq 2$ is complicated by the coupling among dimensions and still remains an open problem.

This material is based upon research supported by, or in part by, the U.S. Office of Naval Research under award number N00014-21-1-2410.

[1]Authors are with the Department of Mechanical Engineering, 2181 Glenn L. Martin Hall, Building 088, University of Maryland, College Park, MD 20742, USA. Email: xxu0116@umd.edu, yancy@umd.edu.

[2]Author is with the Department of Mechanical Engineering and the Center for Control, Dynamical Systems, and Computation, University of California, Santa Barbara, CA 93106, USA. davydov@ucsb.edu.

In this paper, we seek to bridge two popular classes of distributed algorithms of swarm robotics once considered inherently different, i.e., coverage over time-varying domains and leader-follower consensus network. In a coverage control setting, we consider the agents in the domain of interest to be followers while the points that define the boundary of the domain of interest implicitly become leaders. More concretely, we reflect the boundary agents, i.e., the agents whose Voronoi cells share faces with the boundary of the domain of interest, to obtain virtual leader agents. The followers' dynamics in consensus form are provided under the general density cases, as well as the closed-form expressions of followers' and leaders' dynamics under uniform density. Moreover, the ensemble form of the leader-follower network is obtained as a weighted, state-dependent graph Laplacian matrix. The structure and weights of the graph Laplacian, whose topology is that of a Delaunay triangulation, may contribute to the goal of ultimately obtaining tracking error bounds and robustness guarantees of Lloyd's algorithm for coverage over 2D time-varying domains.

The organization of this paper is as follows: Section II introduces MAS coverage control and some lemmas regarding geometry of triangles and polygons. Section III provides an equivalence between Lloyd's algorithm and a leader-follower consensus network. The simulation results are presented in Section IV, and finally the conclusions and discussions about future work are presented in Section V.

II. Preliminaries

In this section, we provide some preliminary descriptions of the coverage control problem in d-dimension and other geometrical results for further investigations on MAS coverage over 2D polygonal domains.

A. The MAS Coverage Problem

Let X be a set of agents, and $|X| = N$; with a slight abuse of notation, let $X(t) = \left[x_1^T(t), \ldots, x_N^T(t)\right]^T \in \mathbb{R}^{Nd}$ also denote the configuration of the multi-agent team at time t, where $x_i(t) \in \mathcal{D}(t) \subseteq \mathbb{R}^d$ is the position of the i^{th} agent in the convex time-varying domain of interest $\mathcal{D}(t)$ at time t. Let $\partial\mathcal{D}(t)$ denote the boundary of the domain at time t.

The objective of the coverage problem is to optimally distribute a team of agents in a domain $\mathcal{D}(t)$ with a density function ϕ defined over $\mathcal{D}(t)$. The modified locational cost

[1] for adapting time-varying densities [13] or domains [14] is used as a metric of the coverage performance in the domain $\mathcal{D}(t)$ at time t:

$$\mathcal{H}(X(t),t) = \sum_{i=1}^{N} \int_{V_i(X(t),t)} \|x_i(t) - q\|^2 \phi(q,t)\, dq \tag{1}$$

where $\phi : \mathcal{D}(t) \times [0,\infty) \to (0,\infty)$ is a density function that captures the relative importance of the points in the domain at time t, and is assumed to be continuously differentiable in both arguments. The domain is partitioned into regions of dominance that form a proper partition of the subdomain. We utilize a Voronoi tessellation of the domain, where agent i's Voronoi cell at time t is given by

$$V_i(X(t),t) = \left\{ q \in \mathcal{D}(t) \middle| \|x_i(t) - q\| \le \left\|x_j(t) - q\right\| \ \forall j \right\}. \tag{2}$$

The Voronoi tessellation of a set of *seed* points X is dual to the Delaunay triangulation of the same points [15]. For ease of notation we henceforth drop the explicit time dependency on the configuration of the multi-agent system.

1) Centroidal Voronoi Tessellations: A necessary condition for minimizing the locational cost in (1) is known to be that the agents form a centroidal Voronoi tessellation (CVT) of the domain [1], i.e., $x_i(t) = c_i(X,t), \forall i,t$ where we define $c_i(X,t) \in V_i(X,t)$ to be the *center of mass* (or centroid) of Voronoi cell i at time t, given by

$$c_i(X,t) = \int_{V_i(X,t)} q\phi(q,t)\, dq \Big/ m_i(X,t) \tag{3}$$

where $m_i(X,t)$ is the mass of the corresponding cell,

$$m_i(X,t) = \int_{V_i(X,t)} \phi(q,t)\, dq. \tag{4}$$

2) Coverage Control Law: In [5] and [13], a control law was proposed to achieve exponential converge to a CVT in the case of time-varying densities or domains. This control law was called TVD-C for *time-varying densities (domains), centralized case*, and its decentralized version was also developed which is called TVD-D_1, stands for *time varying densities (domains), decentralized case with 1-hop adjacency information*. In this paper we are interested in the continuous-time version of Lloyd's algorithm [2], which can be shown to be a gradient descent strategy for minimizing (1) for static cases:

$$\dot{X}(t) = \kappa\left(C(X(t),t) - X(t)\right), \tag{5}$$

where $C(X,t) = \left[c_1(X,t)^T, \ldots, c_N(X,t)^T\right]^T$ as defined in (3) and $\kappa > 0$ is a control gain.

In what follows, we focus on $d = 2$, i.e., planar coverage control. Before investigating the connection between 2D coverage and consensus protocol, we provide a few results of geometry which will be used later.

B. Circumcenter of A Triangle

A well-known fact is that the Voronoi tessellation and Delaunay graph are dual to one another, and the vertices of the Voronoi tessellations in 2D are the circumcenters of the Delaunay triangles in the Delaunay graph [15].

Consider a triangle $\triangle$ whose vertices and corresponding angles are expressed as tuples $\{x_a, x_b, x_c\}$ and $\{\rho_a, \rho_b, \rho_c\}$ respectively (ordered counter-clockwise). Let $x_{ab} = x_b - x_a$. The circumcenter of the triangle, v_{abc}, can be expressed in two different ways [16].

Define the function $f : \triangle \to \mathbb{R}^2$, which maps a triangle to its circumcenter in $\mathbb{R}^2$. Then f can be expressed as

$$v_{abc} = f(\triangle) = \beta_a(\triangle)x_a + \beta_b(\triangle)x_b + \beta_c(\triangle)x_c, \tag{6}$$

where $\beta_a(\triangle) = \mu_a/\nu$, $\beta_b(\triangle) = \mu_b/\nu$, and $\beta_c(\triangle) = \mu_c/\nu$; the first way to obtain these βs is

$$\nu = 2\|x_{ab}\|^2\|x_{bc}\|^2 - 2(x_{ab}^T x_{bc})^2, \ \mu_a = \|x_{bc}\|^2 x_{ab}^T x_{ac},$$

$$\mu_b = \|x_{ac}\|^2 x_{ab}^T x_{cb}, \quad \mu_c = \|x_{ab}\|^2 x_{ac}^T x_{bc}.$$

The second way to find βs is

$$\nu = \sin 2\rho_a + \sin 2\rho_b + \sin 2\rho_c, \tag{7}$$

$$\mu_a = \sin 2\rho_a, \quad \mu_b = \sin 2\rho_b, \quad \mu_c = \sin 2\rho_c. \tag{8}$$

One can find the following property directly from the summation of the βs using (6), (7), and (8).

Lemma 1 ([16]): The circumcenter of a triangle $\triangle$ with vertices $\{x_a, x_b, x_c\}$ and angles $\{\rho_a, \rho_b, \rho_c\}$ is a linear combination of its vertices' positions.

C. Mass and Centroid of 2D Convex Polygons

The mass and center of mass of a 2D convex polygon under uniform density (i.e., when the mass of the polygon is uniformly distributed over its entire surface) can be obtained by triangulating the polygon. Without loss of generality, we let a 2D convex polygon P be defined by its n vertices $\{v_1, v_2, \cdots, v_n\}$ in a counter-clockwise (c.c.w.) order, which ensures that the determinant computation used to find the area of a triangle is positive, and thus the use of the absolute value is omitted. Note the convention does not affect the calculation of the centroid, since negative signs are cancelled when dividing by the mass.

Pick any point $q \in P$ and connect q and all the vertices of P; a triangulation is obtained which contains a set of n triangles $\{\triangle_{qv_1v_2}, \triangle_{qv_2v_3}, \cdots, \triangle_{qv_nv_1}\}$ in a c.c.w. order. From [17], the centroids of the triangles are

$$c^b_{qv_iv_{i+1}} = q + \frac{1}{3}\Big((v_i - q) + (v_{i+1} - q)\Big), \tag{9}$$

and the areas of these triangles are

$$A_{qv_iv_{i+1}} = \frac{1}{2}(v_{i+1} - q)^T S(v_i - q), \tag{10}$$

where $i = 1, \cdots, n$, $v_{n+1} = v_1$, and $S = \left[\begin{smallmatrix} 0 & -1 \\ 1 & 0 \end{smallmatrix}\right]$ which rotates a vector 90° c.c.w.

Thus, for $\phi(q,t) = 1\ \forall t$, by the shoelace formula [17], the mass and the centroid of the polygon are,

$$m_P = \sum_{i=1}^{n} A_{qv_iv_{n+1}}, \quad c_P = \frac{1}{m_P}\sum_{i=1}^{n} A_{qv_iv_{i+1}} c^b_{qv_iv_{i+1}}. \tag{11}$$

We then have

$$c_P = \frac{1}{m_P}\sum_{i=1}^{n} A_{qv_iv_{i+1}}\left[q + \frac{1}{3}\Big((v_i - q) + (v_{i+1} - q)\Big)\right].$$

Expanding the equation, and given that the vertices and triangles are placed in a circular arrangement, we have

$$\begin{aligned} c_P &= q + \frac{1}{3m_P}\sum_{i=1}^{n} A_{qv_iv_{i+1}}(v_i - q) + \frac{1}{3m_P}\sum_{i=1}^{n} A_{qv_{i-1}v_i}(v_i - q) \\ &= q + \frac{1}{3m_P}\sum_{i=1}^{n}\left(A_{qv_iv_{i+1}} + A_{qv_{i-1}v_i}\right)(v_i - q). \end{aligned}$$

We put the expressions derived from the Shoelace formula above together in the following lemma.

Lemma 2 ([17]): Given a 2D convex polygon P defined by its n vertices $\{v_1, v_2, \cdots, v_n\}$ in a c.c.w. order. The centroid of polygon P, denoted as c_P, can be found as

$$c_P = q + \sum_{i=1}^{n} \alpha_i(v_i)(v_i - q), \tag{12}$$

where

$$\alpha_i(v_i) = \frac{1}{3m_P}\left(A_{qv_iv_{i+1}} + A_{qv_{i-1}v_i}\right), \tag{13}$$

q is any point in P, and m_P is the mass of P defined in (11).

Then, we find the following property,

Lemma 3: The center of mass of a 2D convex polygon P can be expressed as (12) where $\alpha_i > 0$, and the α_i can be viewed as linear combination coefficients for the vectors $(v_i - q)$ with the property

$$\sum_{i=1}^{n} \alpha_i(v_i) = \frac{2}{3}. \tag{14}$$

Proof: From the expression of α_i in (13), one can note that $0 < \alpha_i(v_i) < 1$ since it is a ratio that related to the areas of triangles and the mass of the polygon. Additionally, summing $\alpha_i(v_i), i = 1, \cdots, n$ up, we can find that

$$\sum_{i=1}^{n} \alpha_i(v_i) = \frac{1}{3m_P}\left(\sum_{i=1}^{n} A_{qv_iv_{i+1}} + \sum_{i=1}^{n} A_{qv_{i-1}v_i}\right).$$

Since the vertices and triangles are placed in a circular arrangement c.c.w., we conclude that,

$$\sum_{i=1}^{n} \alpha_i(v_i) = \frac{1}{3m_P}(m_P + m_P) = \frac{2}{3}.$$

■

III. 2D Coverage v.s. Consensus Protocol

In this section, we present the equivalence of Lloyd's algorithm (5) for coverage control over a 2D domain $\mathcal{D}(t)$ and the leader-follower consensus protocol. Let the boundary of the polygonal domain $\partial\mathcal{D}(t)$ be composed of m vertices in a c.c.w. order, i.e., $\partial\mathcal{D}(t) = \{d_\ell\}_{\ell=1}^{m}$ and $d_{m+1} = d_1$. Intuitively, the behavior of an agent is such that it coordinates its motion with its neighboring agents in the team and contributes to the optimality of the coverage tasks over a time-varying domain. This could be viewed as an agent attempting to maintain reasonable distances from its neighbors meanwhile it captures the motion of the boundary of the domain. At some level, this behavior resembles the *Boids* [18] which simulates the flocking behavior of birds, where the vertices of $\partial\mathcal{D}(t)$ can be viewed as leader agents, and the agents X are followers. Additionally, after performing a Voronoi tessellation of $\mathcal{D}(t)$, the vertices of the domain $\{d_\ell\}_{\ell=1}^{m}$ will be part of the vertices of Voronoi cells; and, as mentioned earlier, the vertices of a Voronoi diagram are circumcenters of the triangles of its dual, the Delaunay graph. Specifically, we introduce the idea of reflecting the boundary agents with respect to the corresponding portion of $\partial\mathcal{D}(t)$ to create a group of virtual agents (as shown in Fig. 1) such that the vertices of $\mathcal{D}(t)$ can be expressed by circumcenters of Delaunay triangles, and the virtual agents will be viewed as virtual leaders in such a network.

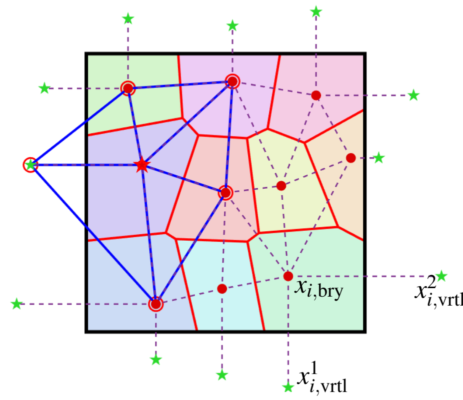

Fig. 1. Geometric illustration of Voronoi tessellation and reflecting boundary agents X_{bry}. For any $x_{i,\text{bry}} \in X_{\text{bry}}$, by reflecting its position with respect to each face of $V_{x_{i,\text{bry}}}(X) \cap \partial\mathcal{D}$ virtual agents will be obtained, e.g., $x^1_{i,\text{vrtl}}$ and $x^2_{i,\text{vrtl}}$ in this figure. Moreover, red "•" denotes real (follower) agents; green "★" denotes virtual (leader) agents; dashed line "- -" denotes adjacency information of real agents; red "★" denotes an agent $x_i \in X$ of interest, and red "∘" denotes x_i's neighbors $x_j \in \mathcal{N}_i$; the Delaunay triangulation over $x_i \cup \mathcal{N}_i$ is marked in blue.

A. Reflecting The Boundary Agents

Consider a set of N agents $X(t) \in \mathcal{D}(t)^N$ where the domain $\mathcal{D}(t)$ is partitioned based on $X(t)$ using a Voronoi tessellation which results in a Voronoi partition $\{V_i(X,t)\}_{i=1}^{N}$. The set X is divided into to two categories X_{int} (i.e., interior agents) and X_{bry} (i.e., boundary agents):

$$X_{\text{int}} = \{x_i \in X \,|\, \mu_{d-1}(V_i(X) \cap \partial\mathcal{D}) = 0, \forall i\}, X_{\text{bry}} = X \backslash X_{\text{int}},$$

where $\mu_{d-1}(A) = 0$ denotes a measure-zero set in a $(d-1)$ sense (in the 2D case, A is a 1D set that is either the empty set or a collection of singletons).

For any $x_i \in X_{\text{bry}}$, by reflecting its position with respect to each face of $V_i(X) \cap \partial\mathcal{D}(t)$ a group of virtual agents X_{vrtl} will be obtained (see Fig. 1). Now computing the Voronoi diagram for all seeds $X_{\text{ttl}} = X \cup X_{\text{vrtl}}$, we have now over $\mathbb{R}^2$,

$$V_i(X_{\text{ttl}}) = \{q \in \mathbb{R}^2 \,|\, \|q - x_i\| \leq \|q - x_j\|, \forall x_j \in X_{\text{ttl}}\}. \tag{15}$$

Remark 1: Performing Voronoi tessellation over $\mathbb{R}^2$ for seeds X_{ttl} as in (15), the Voronoi cells V_i for $x_i \in X$ will be identical to those obtained from (2); and the vertices of the domain $\mathcal{D}$ can be expressed by the circumcenters of the corresponding Delaunay triangles formed by agents in X_{bry} and virtual agents in X_{vrtl}. The reflection will eliminate the inconsistency in the expressions of vertices of Voronoi cells of boundary agents.

B. Leader-Follower Consensus Over Delaunay Graphs

In this section, we will discuss the equivalence of Lloyd's algorithm for coverage control and a leader-follower consensus network.

1) Followers' Dynamics: Let $G=(V,E)$ be the Delaunay graph with generators $V=X_{\text{ttl}}$. For an agent $x_i \in X$, define its Delaunay graph neighbor set as $\mathcal{N}_i=\{x_j \in X_{\text{ttl}} \,|\, (x_i,x_j)\in E\}$; the neighbors are assumed to be arranged in a c.c.w. order, and $x_{j=|\mathcal{N}_i|+1}=x_{j=1}$; and denote $\overline{X}_i=\{x_i\}\cup\mathcal{N}_i$ (Note: $x_i \in X$, but $x_j\in\mathcal{N}_i\subseteq X_{\text{ttl}}$). Then, the Delaunay trianglation over $\overline{X}_i$ returns a set of triangles $\triangle^i=\{\triangle^i_1,\triangle^i_2,\cdots,\triangle^i_{|\mathcal{N}_i|}\}$.

Further define an undirected graph $G^{\triangle}_i=(V^{\triangle}_i,E^{\triangle}_i)$ with no self-loops (see Fig. 2), where $V^{\triangle}_i=\triangle^i$ and

$$E^{\triangle}_i=\{(\triangle^i_k,\triangle^i_\ell)\,|\,\mu_{d-1}\left(\triangle^i_k\cap\triangle^i_\ell\right)\neq 0,\forall\triangle^i_k,\triangle^i_\ell\in\triangle^i\}.$$

One can find that $G^{\triangle}_i$ is a cycle graph geometrically. If we further assign a c.c.w. orientation on the cycle graph, then we can get information of out-neighbors and in-neighbors in the graph. As shown in Fig. 2, for $\triangle^i_j=\{x_i,x_j,x_k\}$, i.e., a tuple of j-th triangle's vertices in c.c.w. order. It has two neighbors, and let us denote its out-neighbor $\overline{\triangle^i_j}=\triangle^i_k=\{x_i,x_k,x_\ell\}$ (it takes information of $\triangle^i_j$ in $G^{\triangle}_i$) and its in-neighbor $\underline{\triangle^i_j}=\triangle^i_h=\{x_i,x_h,x_j\}$ (it feeds information to $\triangle^i_j$ in $G^{\triangle}_i$). Moreover, as defined in Section II-B, for the triangle $\triangle^i_j$, the function f, returns the circumcenter of this triangle, i.e., $f(\triangle^i_j)=v^i_j$ which also is the j-th vertex of x_i's Voronoi cell.

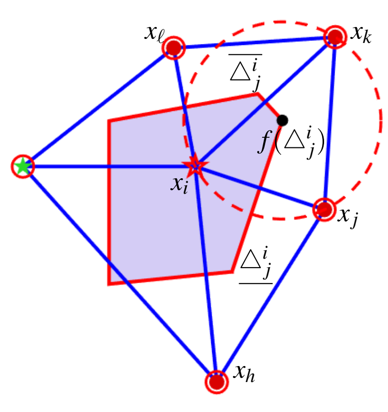

Fig. 2. A zoomed-in view of Delaunay triangulation and Voronoi cell of $x_i\cup\mathcal{N}_i$. The Delaunay triangulation and the Voronoi cell V_i over $x_i\cup\mathcal{N}_i$ are marked in blue and red respectively. Red "★" denotes an agent $x_i\in X$ of interest, and red "○" denotes x_i's neighbors $x_j\in\mathcal{N}_i$. The vertices of the Voronoi cell V_i, e.g., $f(\triangle^i_j)$, are the circumcenters of the Delaunay triangles, e.g., $\triangle^i_j=\{x_i,x_j,x_k\}$. Additionally, these Delaunay triangles are seeds of the graph $G^{\triangle}_i$; with a c.c.w. orientation assigned, $\triangle^i_j$ has one out-neighbor $\overline{\triangle^i_j}$ and one in-neighbor $\underline{\triangle^i_j}$.

Theorem 1 (Followers' Dynamics (General Density)): Given a set of agents $X(t)$ in a domain $\mathcal{D}\subset\mathbb{R}^2$, the continuous-time version of Lloyd's algorithm (as defined in (5)) for MAS coverage control under general density cases, i.e., $\dot{x}_i(t)=\kappa\left(c_i(X,t)-x_i(t)\right),\forall x_i\in X$, is equivalent to a leader-follower consensus protocol

$$\dot{x}_i=\sum_{j\in\mathcal{N}_i}\omega_{ij}(X_{\text{ttl}},t)(x_j-x_i), \tag{16}$$

where $x_i\in X$, $x_j\in X_{\text{ttl}}$, and

$$\omega_{ij}=\kappa\sigma^i_j(t)\left(\alpha^i_j(f(\triangle^i_j))\,\beta^i_b(\triangle^i_j)+\alpha^i_j(f(\underline{\triangle^i_j}))\,\beta^i_c(\underline{\triangle^i_j})\right) \tag{17}$$

with $\sigma^i_j(t)>0$; the $\beta(\cdot)$s and $\alpha^i(\cdot)$ defined in (6) and (13).

Proof: For the set of agents $\overline{X}_i=\{x_i\}\cup\mathcal{N}_i$ and the resultant Delaunay triangles $\triangle^i$. The circumcenters of these triangles, i.e., $\{f(\triangle^i_j)\}^{|\mathcal{N}_i|}_{j=1}$, are the vertices of the Voronoi cell $V_i(X)$. Carathéodory's theorem [19] suggests that any point inside a polygon can be expressed as the convex combination (with strictly positive coefficients, without loss of generality) of the vertices of this polygon, and the coefficients for the convex combination are not unique. Therefore, for agent i's polygonal Voronoi cell $V_i(X)$, its centroid c_i can be anywhere inside it under general density $\phi(q,t)$, and there exist real numbers $\lambda^i_j(f(\triangle^i_j),\phi(q,t))>0$ and $\sum^{|\mathcal{N}_i|}_{j=1}\lambda^i_j=1$ at every time t such that

$$c_i=\sum^{|\mathcal{N}_i|}_{j=1}\lambda^i_j(f(\triangle^i_j),\phi(q,t))\,f(\triangle^i_j).$$

Further we assume that the position of Voronoi cell $V_i(X)$ moves away from the origin by a quantity x_i in the space, then the centroids will shift by the same quantity, we have

$$c_i-x_i=\sum^{|\mathcal{N}_i|}_{j=1}\lambda^i_j(f(\triangle^i_j),\phi(q,t))\,(f(\triangle^i_j)-x_i).$$

Comparing this to the result in Lemma 2 under uniform density, with $0<\alpha^i_j(f(\triangle^i_j))<1$ from Lemma 3, we conclude that for every time t there exist real numbers $\sigma^i_j(t)>0$ such that $\sigma^i_j(t)\,\alpha^i_j=\lambda^i_j(f(\triangle^i_j),\phi(q,t))$.

Further, the Lloyd's algorithm can be written as

$$\begin{aligned}\dot{x}_i&=\kappa(c_i-x_i)=\kappa\sum^{|\mathcal{N}_i|}_{j=1}\sigma^i_j(t)\alpha^i_j(f(\triangle^i_j))\left(f(\triangle^i_j)-x_i\right)\\&=\kappa\sum^{|\mathcal{N}_i|}_{j=1}\sigma^i_j\alpha^i_j(\triangle^i_j)\left(\beta^i_a(\triangle^i_j)x_i+\beta^i_b(\triangle^i_j)x_j+\beta^i_c(\triangle^i_j)x_k-x_i\right).\end{aligned}$$

From Lemma 1 we have that $\beta^i_a(\triangle^i_j)-1=-\beta^i_b(\triangle^i_j)-\beta^i_c(\triangle^i_j)$, thus,

$$\begin{aligned}\dot{x}_i=\kappa\Bigg(&\sum^{|\mathcal{N}_i|}_{j=1}\sigma^i_j(t)\alpha^i_j(f(\triangle^i_j))\,\beta^i_b(\triangle^i_j)\,(x_j-x_i)\\&+\sum^{|\mathcal{N}_i|}_{j=1}\sigma^i_j(t)\alpha^i_j(f(\triangle^i_j))\,\beta^i_c(\triangle^i_j)\,(x_k-x_i)\Bigg)\end{aligned}$$

since the vertices and triangles are placed in a circular arrangement c.c.w., we have

$$\dot{x}_i = \kappa \sum_{j=1}^{|\mathcal{N}_i|} \sigma_j^i(t) \Bigg(\alpha_j^i(f(\triangle_j^i))\beta_b^i(\triangle_j^i) + \alpha_j^i(f(\underline{\triangle_j^i}))\beta_c^i(\underline{\triangle_j^i}) \Bigg) (x_j - x_i)\,,$$

which yields (16) and (17), and

$$\begin{aligned} \alpha_j^i(f(\triangle_j^i)) &= \frac{1}{3m_i}\left(A^b_{x_i f(\triangle_j^i) f(\overline{\triangle_j^i})} + A^b_{x_i f(\underline{\triangle_j^i}) f(\triangle_j^i)} \right), \\ \alpha_j^i(f(\underline{\triangle_j^i})) &= \frac{1}{3m_i}\left(A^b_{x_i f(\underline{\triangle_j^i}) f(\triangle_j^i)} + A^b_{x_i f(\underline{\underline{\triangle_j^i}}) f(\underline{\triangle_j^i})} \right), \\ m_i &= \sum_{j=1}^{|\mathcal{N}_i|} A^b_{x_i f(\triangle_j^i) f(\overline{\triangle_j^i})}. \end{aligned}$$

■

Under general density cases, the coefficients for the convex combination $\lambda_j^i > 0,\ j = 1, \cdots, |\mathcal{N}_i|$ are not unique, thus, the same can be said about the σ_j^is. These coefficients make the expressions of weights $\omega_{ij}(X_{\text{ttl}}, t)$ ambiguous. However, for the uniform density cases, the closed form of expressions of weights $\omega_{ij}(X_{\text{ttl}}, t)$ can be made explicit.

Theorem 2 (Followers' Dynamics (Uniform Density)): Given a set of agents $X(t)$ in a domain $\mathcal{D} \subset \mathbb{R}^2$, the continuous-time version of Lloyd's algorithm for MAS coverage control under uniform density cases, i.e., $\dot{x}_i(t) = \kappa(c_i(t) - x_i(t)), \forall x_i \in X$, can be formulated into a leader-follower consensus protocol shown in (16) with weights (17) where $\sigma_j^i(t) = 1, \forall j, \forall t$.

Proof: Follows directly from Theorem 1. ■

Now let us take a look at virtual leaders' dynamics.

2) Leaders' Dynamics: As introduced in Section III-A, for a bounday agent $x_{i,\text{bry}} \in X_{\text{bry}}$, its Voronoi cell $V_{x_{i,\text{bry}}}(X)$ will partially share boundaries with $\partial\mathcal{D}$, i.e.,

$$\{\partial\mathcal{D}\}_{x_{i,\text{bry}}} = \{(d_\ell, d_{\ell+1}) \in \partial\mathcal{D} \mid \mu_{d-1}\left(\partial\mathcal{D} \cap V_{x_{i,\text{bry}}}(X)\right) \neq 0, \forall \ell\}.$$

Hence, for each line-segment boundary between the pair of vertices $(d_\ell, d_{\ell+1})$, there is a a virtual agent $x_{i,\text{vrtl}}^\ell$ which is created by reflecting $x_{i,\text{bry}}$ with respect to a line (hyperplane) $(d_\ell, d_{\ell+1})$. Perceivably, the dynamics of the virtual leaders consist of two portions, i.e., the dynamics of their corresponding boundary agents and the dynamics of the domain. Thus, we have the dynamics of the virtual leader agents as follows.

Theorem 3 (Virtual Leaders' Dynamics): With the formulation stated in Section III, the dynamics of the virtual leaders are

$$\dot{x}_{i,\text{vrtl}}^\ell = \pi_\ell \dot{x}_{i,\text{bry}} + (I_2 - \pi_\ell)\dot{d}_\ell + \dot{\pi}_\ell \left(x_{i,\text{bry}} - d_\ell\right), \qquad (18)$$

$\forall (d_\ell, d_{\ell+1}) \in \{\partial\mathcal{D}\}_{x_{i,\text{bry}}}$, where $\pi_\ell = I_2 - 2\hat{n}_\ell\hat{n}_\ell^T$; I_2 is a $[2\times 2]$ identity matrix; $\hat{n}_\ell = S\hat{d}_\ell / \|\hat{d}_\ell\|$ denotes the unit normal vector of line $(d_\ell, d_{\ell+1})$ by defining $\hat{d}_\ell = d_{\ell+1} - d_\ell$. Moreover, $\dot{\pi}_\ell = -2\dot{\hat{n}}_\ell\hat{n}_\ell^T - 2\hat{n}_\ell\dot{\hat{n}}_\ell^T$; and $\dot{\hat{n}}_\ell = \left(\|\hat{d}_\ell\| S - \hat{n}_\ell \hat{d}_\ell^T\right)\dot{\hat{d}}_\ell / \|\hat{d}_\ell\|^2$.

Proof: The Householder transform [20] is a linear transformation that describes a reflection about a plane or hyperplane containing the origin, thus given a hyperplane $(d_\ell, d_{\ell+1})$ and a point $x_{i,\text{bry}}$, its corresponding virtual agents is given by $x_{i,\text{vrtl}}^\ell = \pi_\ell\left(x_{i,\text{bry}} - d_\ell\right) + d_\ell$. By taking the derivative, the dynamics of virtual leaders follow. ■

C. Ensemble Form

Let us arrange $\mathbf{x} = [X^T, X_{\text{vrtl}}^T]^T$ where $|X| = N$, $|X_{\text{vrtl}}| = M$. From the dynamics (16), (17), and (18) we can define a weighted-Laplacian-like matrix

$$\mathcal{L}_\omega(X_{\text{ttl}}, t) = \begin{pmatrix} \left[\mathcal{L}_\omega^f\right]_{[N\times N]} & [\ell_\omega]_{[N\times M]} \\ 0_{[M\times N]} & 0_{[M\times M]} \end{pmatrix}, \qquad (19)$$

then, we have a leader-follower consensus network,

$$\dot{X}(t) = \kappa\Bigg(-\left(\mathcal{L}_\omega^f(X_{\text{ttl}}, t) \otimes I_2\right) X(t) - \left(\ell_\omega(X_{\text{ttl}}, t) \otimes I_2\right) X_{\text{vrtl}}(X, t)\Bigg), \qquad (20)$$

where $\otimes$ denotes Kronecker product, and

$$\left[\mathcal{L}_\omega^f\right]_{ij} = \begin{cases} \sum_{j\in\mathcal{N}_i\subseteq X_{\text{ttl}}} \omega_{ij}(X_{\text{ttl}}, t), & i = j,\ j \in X_{\text{ttl}} \\ -\omega_{ij}(X_{\text{ttl}}, t), & i \neq j,\ j \in X \end{cases} \qquad (21)$$

$$[\ell_\omega]_{ij} = -\omega_{ij}(X_{\text{ttl}}, t), \qquad i \neq j,\ j \in X_{\text{vtl}} \qquad (22)$$

and the leaders' dynamics $\dot{X}_{\text{vrtl}}(t)$ can be obtained from (18).

The Laplacian matrix with nonlinear, state-dependent, and time-varying weights in (21) degenerates to a matrix with linear time-invariant entries for coverage control over 1D manifolds [11], and this property contributes to the establishment of the bounds on error dynamics of tracking time-varying manifolds. However, the discussion about the robustness guarantees of decentralized coverage algorithms over time-varying domains in 2D falls outside of the scope of the main objective considered in this paper. We aim to show the equivalence of 2D coverage control using Lloyd's algorithm and leader-follower consensus network, and these results, e.g., the dimension-independent graph Laplacian matrix of the Delaunay graph with its properties, will serve as preliminaries of investigation of the performance bounds of decentralized coverage control.

IV. Simulations

In this section, we validate the equivalence between the two algorithms, i.e., the Lloyd's algorithm for coverage control (5) and the leader-follower consensus network (20), in simulations. Implementing collision avoidance is necessary for MAS controls, and it can be done by various approaches, such as potential field, edge-tension function, etc. Although we do not explicitly consider collision avoidance here, MAS coverage naturally achieves safety by spreading agents out over a domain.

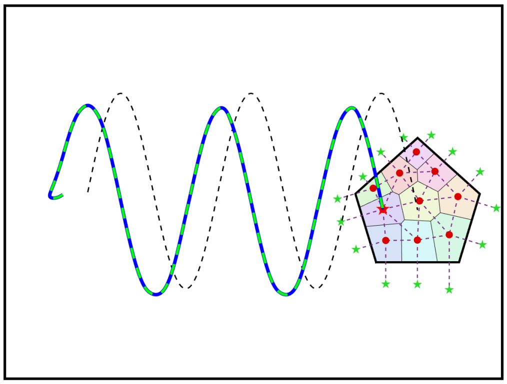

Fig. 3. Simulation results by implementing Lloyd's algorithm (5) and leader-follower consensus protocol (20). A polygon domain is moving along a sinusoidal trajectory, i.e., the black dashed line "- -"; the trajectory of a randomly selected agent (denoted as red "★") is denoted by the blue solid line "–" and green dashed line "- -" when implementing Lloyd's algorithm and leader-follower consensus protocol respectively.

In the simulations of the two algorithms, the initial condition for the polygonal domain and configuration of agents are identical. As shown in Fig. 3, the domain is commanded to move along a sinusoidal trajectory. We randomly select an agent (denoted by a red "★") and visualize the trajectories of this agent when the two algorithms are implemented. The communication topology is the Delaunay graph, which is the dual of the Voronoi diagram, in both algorithms. The blue trajectory is a result of Lloyd's algorithm while the green one is from the leader-follower consensus protocol. We note that the two trajectories overlap with each other which validates the equivalence of these two control laws.

V. Conclusions and Future Work

Conclusions: Reformulation of the distributed coverage control algorithm over 2D domains, i.e., Lloyd's algorithm, into a leader-follower consensus network is established. The dynamics of followers (i.e., real agents in MAS) are in a form of weighted, state-dependent consensus protocol on an interaction topology of Delaunay triangulation, where the closed-form expression of the weights are found for uniform density cases; and the dynamics of leaders (virtual agents resulted from reflecting boundary agents with respect to the corresponding faces of the polygonal domain) is provided. A weighted graph Laplacian matrix is obtained from the ensemble dynamics of the leader-follower consensus protocol. The simulations validate the equivalence of the two classes of distributed MAS control algorithms.

Future Work: The leader-follower consensus representation of the 2D coverage control algorithm arranges the ensemble dynamics of a multi-agent system in a more structured way. The weighted, state-dependent graph Laplacian is related to a well-studied topology of interaction, i.e., Delaunay triangulation. The existing properties associated with such a Laplacian matrix may contribute to reasoning about the robustness guarantees on the MAS's coverage performance. By leveraging the structure of graph Laplacian, together with other control theoretic-techniques such as contraction theory [21] and time-varying nonconvex optimization [22], the future plan will be obtaining bounds on the tracking error dynamics of the MAS tracking a reference input encoded through the boundary of the domain of interest in 2D coverage control.

References

[1] J. Cortés, S. Martinez, T. Karatas, and F. Bullo, "Coverage control for mobile sensing networks," *IEEE Transactions on Robotics and Automation*, vol. 20, no. 2, pp. 243–255, April 2004.

[2] S. Lloyd, "Least squares quantization in PCM," *IEEE Transactions on Information Theory*, vol. 28, no. 2, pp. 129–137, 1982.

[3] W.-T. Li and Y.-C. Liu, "Human-swarm collaboration with coverage control under nonidentical and limited sensory ranges," *Journal of the Franklin Institute*, vol. 356, no. 16, pp. 9122–9151, 2019.

[4] Y. Diaz-Mercado, S. G. Lee, and M. Egerstedt, "Human–swarm interactions via coverage of time-varying densities," *Trends in Control and Decision-Making for Human–Robot Collaboration Systems*, pp. 357–385, 2017.

[5] X. Xu and Y. Diaz-Mercado, "Multi-agent control using coverage over time-varying domains," in *American Control Conference (ACC)*, 2020, pp. 2030–2035.

[6] X. Xu, G. Shi, P. Tokekar, and Y. Diaz-Mercado, "Interactive multi-robot aerial cinematography through hemispherical manifold coverage," in *IEEE/RSJ International Conference on Intelligent Robots and Systems (IROS)*, 2022, pp. 11 528–11 534.

[7] S. Lee and Y. Kim, "Distributed persistent coverage control and performance evaluation of multi-agent system," *The Aeronautical Journal*, vol. 123, no. 1268, pp. 1701–1723, 2019.

[8] X. Xu, E. Rodrıguez-Seda, and Y. Diaz-Mercado, "Persistent awareness-based multi-robot coverage control," in *59th IEEE Conference on Decision and Control (CDC)*, 2020, pp. 5315–5320.

[9] Z. Zhou, W. Zhang, J. Ding, H. Huang, D. M. Stipanović, and C. J. Tomlin, "Cooperative pursuit with Voronoi partitions," *Automatica*, vol. 72, pp. 64–72, 2016.

[10] P. Rivera-Ortiz and Y. Diaz-Mercado, "On guaranteed capture in multi-player reach-avoid games via coverage control," *IEEE Control Systems Letters*, vol. 2, no. 4, pp. 767–772, 2018.

[11] A. Davydov, P. Rivera-Ortiz, and Y. Diaz-Mercado, "Pursuer coordination in multi-player reach-avoid games through control barrier functions," *IEEE Control Systems Letters*, vol. 5, no. 6, pp. 1910–1915, 2021.

[12] D. Gu and Z. Wang, "Leader–follower flocking: Algorithms and experiments," *IEEE Transactions on Control Systems Technology*, vol. 17, no. 5, pp. 1211–1219, 2009.

[13] S. G. Lee, Y. Diaz-Mercado, and M. Egerstedt, "Multirobot control using time-varying density functions," *IEEE Transactions on Robotics*, vol. 31, no. 2, pp. 489–493, April 2015.

[14] X. Xu and Y. Diaz-Mercado, "Multi-robot control using coverage over time-varying non-convex domains," in *IEEE International Conference on Robotics and Automation (ICRA)*, 2020, pp. 4536–4542.

[15] F. P. Preparata and M. I. Shamos, *Computational Geometry: An Introduction*. Springer Science & Business Media, 2012.

[16] D. Pedoe, *Circles: A Mathematical View*. Cambridge University Press, 1995.

[17] P. Bourke, "Calculating the area and centroid of a polygon," *Swinburne Univ. of Technology*, vol. 7, 1988.

[18] C. W. Reynolds, "Flocks, herds and schools: A distributed behavioral model," in *Proceedings of the 14th Annual Conference on Computer Graphics and Interactive Techniques*, 1987, pp. 25–34.

[19] C. Carathéodory, "Über den variabilitätsbereich der Fourier'schen konstanten von positiven harmonischen funktionen," *Rendiconti Del Circolo Matematico di Palermo (1884-1940)*, vol. 32, no. 1, pp. 193–217, 1911.

[20] A. S. Householder, "Unitary triangularization of a nonsymmetric matrix," *Journal of the ACM (JACM)*, vol. 5, no. 4, pp. 339–342, 1958.

[21] W. Lohmiller and J.-J. E. Slotine, "On contraction analysis for non-linear systems," *Automatica*, vol. 34, no. 6, pp. 683–696, 1998.

[22] Y. Ding, J. Lavaei, and M. Arcak, "Time-variation in online nonconvex optimization enables escaping from spurious local minima," *IEEE Transactions on Automatic Control*, vol. 68, no. 1, pp. 156–171, 2023.